

# CHAPTER 4

## **The formation of aligned droplets by dewetting of electrospun Polystyrene nanofibers and its comparison with Rayleigh Plateau Instability**

### **Abstract**

In this chapter, aligned and ordered dewetted nanostructures are produced by dewetting of electrospun polymer nanofibers. A major limitation in the previously used method is that dewetting on a flat homogeneous surface produces randomly distributed droplets. Various strategies have been suggested for aligning the droplets by controlled dewetting on physically or chemically patterned substrates or by combining dewetting with other lithography techniques. Here, we had discussed a novel and simple method of producing aligned nanostructures by dewetting of polystyrene nanofibers. The number density of the dewetted nanostructures can also be increased by again depositing nanofibers on the dewetted substrate and dewetting it again with the optimal dewetting mixture.

### **4.1 Introduction**

#### **4.1.1 Basic Theory and Mechanism**

Electrospun polymer fibres are widely employed in applications like filtration [1], tissue engineering [2,3], energy [4], and composites [5,6] where their high surface-to-volume ratio is essential. Due to their relatively high surface area to volume ratio, electrospun fibres have advantages over many other fibrous materials, especially as fibre diameters approach to nanoscale dimensions. When a polymer solution is pulled as a jet by an electric field, Rayleigh-Plateau/Weber instabilities are prominent in the electrospinning process.[7] During electrospinning, the rapid solvent evaporation, which limits polymer chain mobility until solid

polymer is collected, competes with the surface energy-driven instability and break-up into droplets. Recently, similar instability was observed when annealing nanowires at 400–600 °C [8], also while ink-jet printing [9], and techniques for electrospraying liquid and solid particle aerosols [10-13]. If material is able to flow in fibrous geometries, the surface of the cylindrical shape is always initially perturbed. This perturbation can be seen as the initial crests and troughs of a particular wavelength in the fibre topography. The break-up process is initiated by this variation in the topology of the fibre. When the polymer molecules in the polymer have enough mobility, the fibre curvature causes material to move from the crests to troughs, increasing the wave amplitude. The break-up process with the fastest rate is specified by the Rayleigh-Plateau/Weber wavelength.

It was predicted by Plateau more than a century ago that a liquid cylinder with radius  $r$  is unstable to perturbations with radius whose wavelength  $\lambda$  is greater than the cylinder's circumference. The total energy of the cylinder thus decreases by decomposing into an array of spherical droplets under volume conservation.[14] His work was continued with Lord Rayleigh's theoretical investigations on the instability of liquid jets.[15] As of now, a wide range of processes, including the production of water drops, fibre spinning, and the fission of charged finite systems like atomic nuclei or liquid droplets, are based on this Rayleigh instability phenomenon.

The previously used method produces randomly distributed droplets. Various strategies had been adopted for producing ordered and aligned dewetted nanostructures by controlled dewetting on physically or chemically patterned substrates or by combining dewetting with other lithography techniques. However, coating a uniform thickness film on physico-chemically patterned substrates is often difficult, especially coating of very thin (<20 nm) films that are unstable. Further, fabrication of a hard (*e.g.*, silicon) template dedicated to dewetting of a single film is an expensive process. Finally, heterogeneities of the template cannot be

selectively obliterated after patterning of the polymer. Thus, although template mediated dewetting can give ordered polymer arrays as a proof-of-concept, it is not especially attractive for large-scale manufacturing. Further, it is also important to note that polymeric features with smooth circular shapes, such as nano-lenses and their ordered arrays, cannot be directly and easily fabricated with the top-down techniques such as EBL. Therefore, the formation of aligned droplets by dewetting of nanofibers is a simple yet effective method.

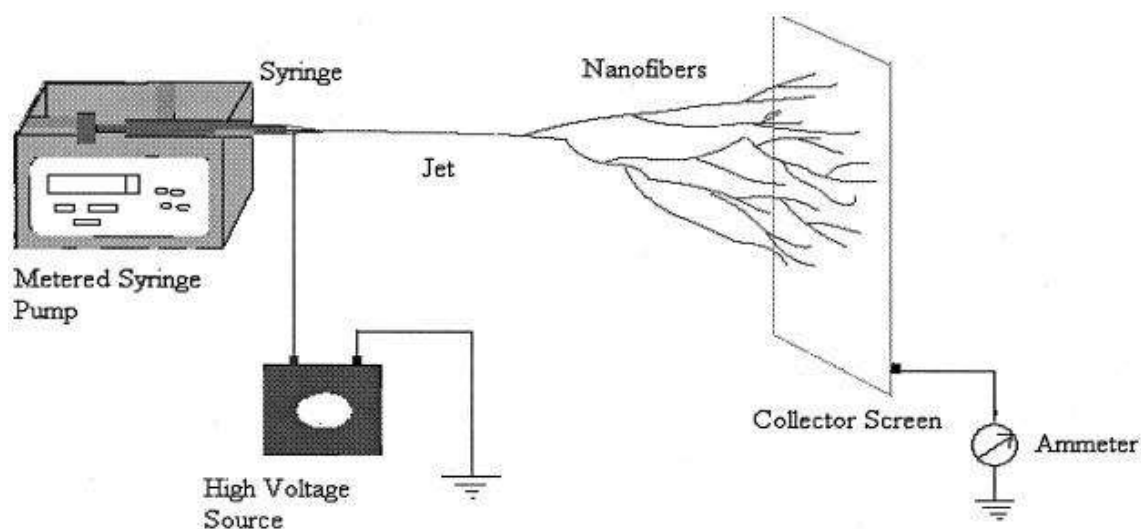


**Figure 26:** Schematic of electrospinning process.

## 4.2 Materials and Method

### 4.2.1 Materials and Chemicals

Polystyrene (PS) of average molecular weight 280 kg/mol procured from Sigma Aldrich, India was used in the experiments. HPLC grade chemicals used Dimethylformamide (DMF), Methyl Ethyl Ketone, toluene, acetone, tetrachloroethylene (TCE), methanol, ammonium hydroxide, hydrogen peroxide, concentrated sulphuric acid were purchased from Merk, Mumbai, India. The materials like glass slide holder, vials, syringe were purchased from M.S. Scientific, India.

## **4.2.2 Equipments**

The equipments used in the present work were electrospinning apparatus, vortex mixer, hot plate, sonicator, laminar flow chamber, hair-dryer.

## **4.2.3 Glasswares**

Beaker, volumetric flask, measuring cylinders, pipette etc. were used which were made with borosilicate glass. Prior to use all glasswares were sterilized with sulphuric acid and potassium dichromate and thereafter rinsed properly with distilled water.

## **4.2.4 Methods**

### **4.2.4.1 Cleaning of glass slides**

The RCA-I cleaning protocol is a detailed multi-step cleaning procedure of silicon wafers developed by Werner Kern at Radio Corporation of America (RCA) laboratories in late 1960s. The silicon wafers were thoroughly cleaned before use in order to remove dust particles and organic contaminants from the substrate. The silicon wafers were cleaned by RCA1 protocol. In this firstly, the silicon wafers were soaked in 10% soap solution. Then the substrates were cleaned by brushing for 1min. for each substrate. Later it was rinsed without froth. Then it is boiled in Trichloroethylene (TCE) solution followed by boiling it into acetone and methanol. 511 solution is prepared by mixing 40 ml ammonium hydroxide, 40 ml of hydrogen peroxide and 200 ml of water in a beaker. The substrates are boiled in this solution at 100°C for half an hour. Pirannah solution a highly oxidizing solution is prepared by mixing 3 parts of concn. Sulphuric acid to 1 part of hydrogen peroxide. The substrates were slowly dipped in this solution and kept for 15 min.

#### **4.2.4.2 Deposition of electrospun Polystyrene fiber**

The equipment for electrospinning comprises of a positive or negative polarity high voltage power source, a needle spinneret coupled to a syringe with a polymer reservoir, and a conducting flat plate or rotating drum acting as a ground collector. The polymer solution or melt is held by its surface tension in the form of a droplet at the needle tip.(figure 26) The pendant droplet of the polymer solution at the needle tip is distorted into a conical shape when an electric potential is supplied between the syringe needle and collector, followed by an increase in voltage, inducing charge on the fluid surface. (Taylor cone) This happens when the surface tension of the polymer solution or melt and the electric forces are in equilibrium. The electrostatic force will enhance the electrical repulsion between the mutual charges on the drop's surface when the electrical field strength exceeds a critical value. The surface tension of the polymer solution will be overcome by the electrostatic forces, and as a result, a fine charged jet will be ejected from the cone's tip. The jet eventually solidifies into fibres that are deposited on the collecting plate as the solvent instantly begins to evaporate in the background. The electrospinning of jet generally involves three phases. The first one is the Taylor cone formation in a liquid drop at the syringe's needle tip. Later, a linear jet appears at the cone's base and travels towards the ground collector. The electrospun jet undergoes bending instability after only a few millimetres at most because of the strong electrostatic forces acting on the jet's surface.[16]

The Taylor cone's tip is the region of bending instability, when the jet bends as a result of strong electrostatic forces acting on its surface. The electrically charged pendant droplet at the needle tip can only take on a stable shape if the electric field is not too strong when applied between the droplet and a ground plate.

The electrically charged pendent droplet at the needle tip can only take on a stable shape if the electric field is not too strong when applied between the droplet and a ground plate. This stable shape appear only when the surface tension of the droplet and electric forces are in equilibrium. When the electrical potential is increased further, this shape is distorted and the droplet takes on the Taylor cone shape. The cone observed in electrospinning from which a jet of charged particles emerges above a threshold voltage is thus referred to as the Taylor cone. After being stretched and moving a certain distance toward the ground electrode, the charged polymer jet experiences a bending (whipping) instability that causes the jet to convert into ultrafine fibres. In particular, nanowires may disintegrate into a chain of nanospheres when heated above a certain temperature.

#### **4.2.4.3 Dewetting procedure**

Annealed PS fibres were placed in dewetting chamber containing optimal mixture of water, MEK and acetone in the ratio 15:7:3. The dewetting is done *in-situ* under the observation of microscope. The dewetting was carried for a fixed period of time i.e., 30 min. The dewetting was carried out at the room temperature. MEK is a good solvent for PS. Diffusion of MEK in PS reduces its glass transition temperature and allow PS to dewett at room temperature. As MEK is a good solvent of PS water is added to limit the solubility of PS into the dewetting solution. Also, water and MEK are sparingly soluble therefore, acetone is added to form a homogeneous mixture. Dewetted structures were examined using an optical microscope (Nikon Eclipse Y-TV55) in bright field mode.(figure 27)

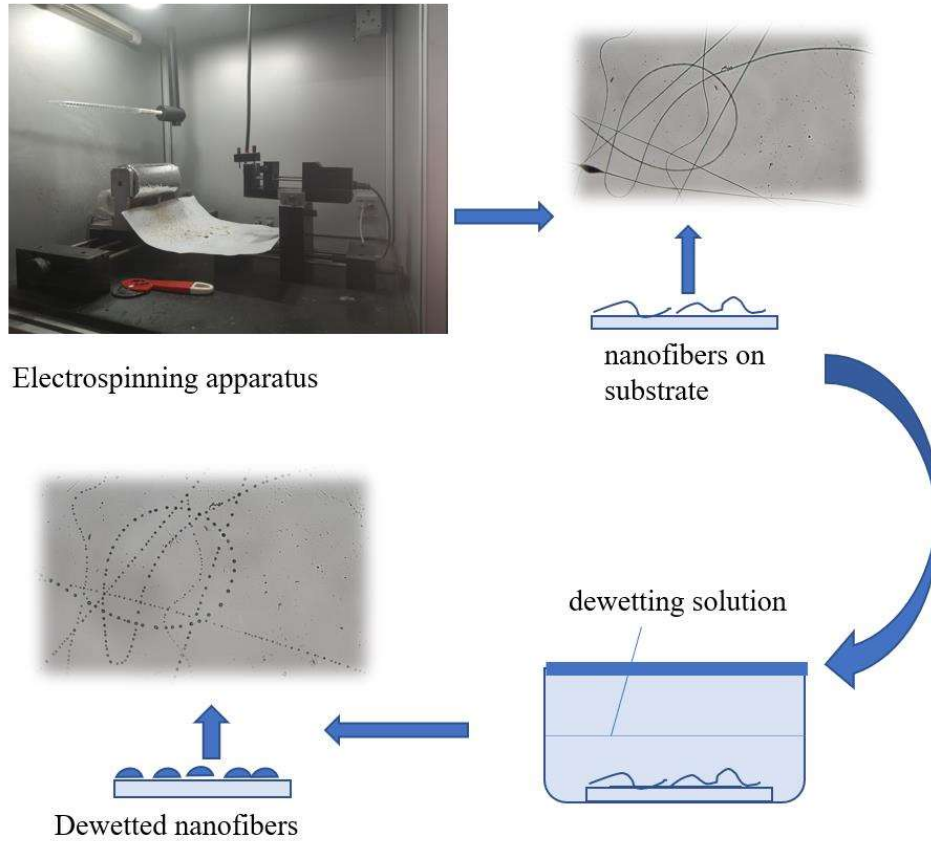


**Figure 27:** Schematic diagram of experimental setup

### 4.3 Results and Discussion

The dewetting of electrospun fibers was carried out at for different conditions by varying annealing temperature and substrate wettability properties. The dewetting of electrospun fibers is studied for following conditions:

- Deposition of fibers on unsilanized substrates and annealed at lower temperature(60°C)
- Deposition of fibers on silanized substrate and annealed at lower temperature (60°C).
- Deposition of fibers on unsilanized substrate and annealing at a higher temperature (120°C).

- Deposition of fibers on silanized substrate and annealing at a higher temperature (120°C)

**Table 2:** Operating parameters

Fiber concentration (%wt.)	8
Voltage used (kV)	12
Flow rate (µl/min)	15
Distance (cm)	11
Deposition time(min.)	2
Syringe diameter(mm)	13.08

**Table 3:** Solution Parameter

<b>Parameters</b>	<b>Effect on fiber morphology</b>
Viscosity	Low-beads generation, high-increase in fiber diameter , disappearance of beads
Polymer concentration	Increase in fiber diameter with increase of concentration.
Molecular weight of Polymer	Reduction in the number of beads and droplets with increase of molecular weight.
Conductivity	Decrease in fiber diameter with increase in conductivity.

**Table 4:** Processing Parameter

<b>Parameters</b>	<b>Effect on fiber morphology</b>
Applied voltage	Decrease in fiber diameter with increase in voltage
Distance between tip and collector	Generation of beads with too small and too large distance, minimum distance required for uniform fibers.
Feed rate/Flow rate	Decrease in fiber diameter with decrease in flow rate, generation of beads with too high flow rate.
Humidity	High humidity results in circular pores on the fibers.

### 4.3.1 Deposition of fibers on unsilanized substrates and annealed at lower temperature(60°C)

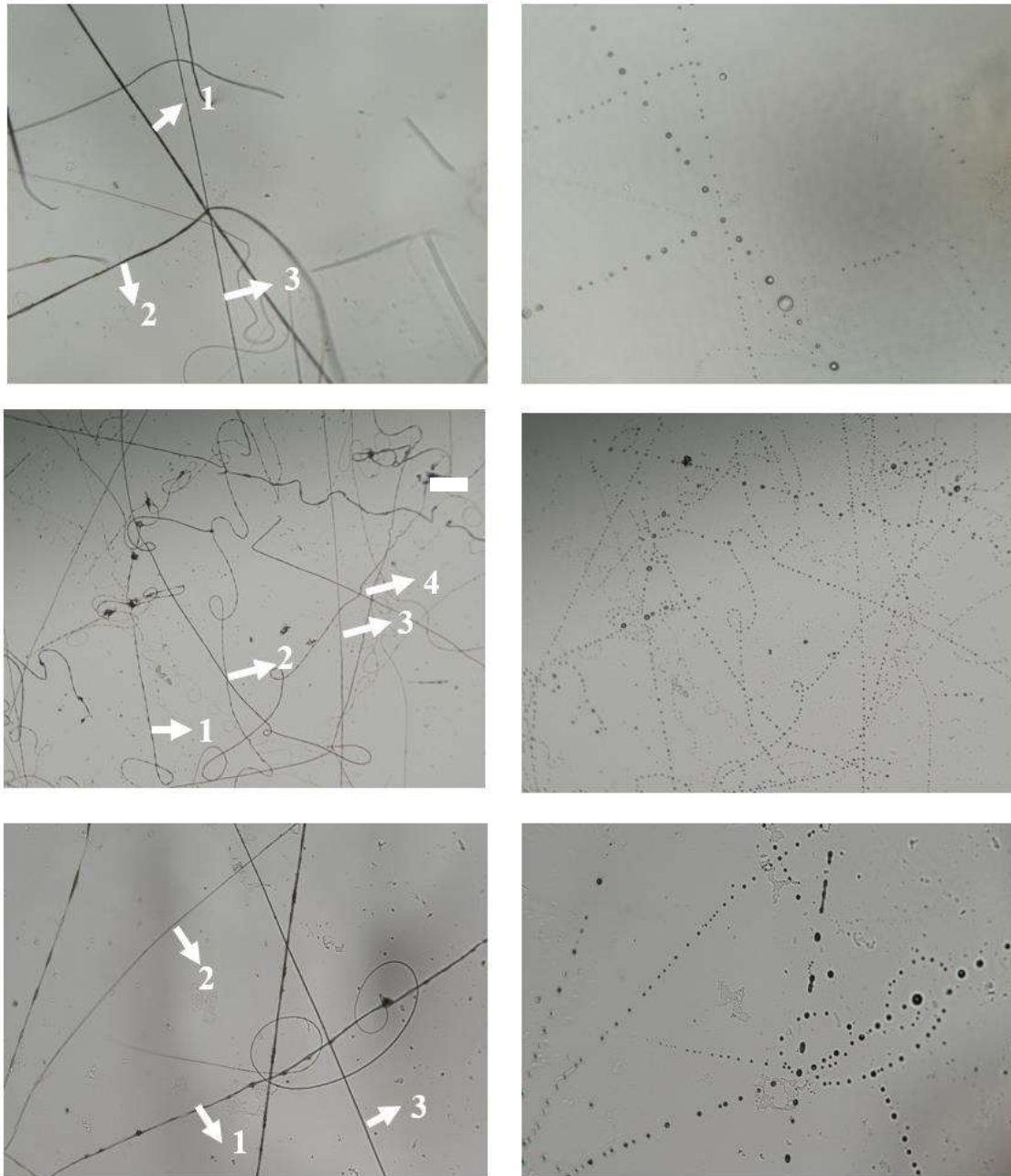


**Figure 29:** In-situ dewetting of nanofibers on unsilanized substrates and annealed at lower temperature(60°C) (Scale:20 $\mu$ m)

**Table 5:** Length-scale parameters for dewetting of nanofibers on unsilanized substrates and annealed at lower temperature(60°C)

<b>Fiber</b>	<b>Wavelength(<math>\lambda</math>)/ <math>\mu\text{m}</math></b>	<b>Droplet diameter/ <math>\mu\text{m}</math></b>	<b><math>\lambda/d</math></b>
<b>4.0±0.4</b>	30.2	6.4	7.6
<b>3.5±0.2</b>	21.8	5.5±2.1	6.2
<b>1.9±0.2</b>	13.5±0.4	3.10±0.4	7.2
<b>1.4±0.3</b>	7.8±1.1	2.2±0.2	5.4
<b>4.0±0.9</b>	8.0±0.5	2.0±0.3	2.0
<b>2.3</b>	6.4±0.9	1.7±0.2	2.8
<b>1.5±0.2</b>	6.3	2.0±0.3	4.2
<b>2.7±0.6</b>	17.5±3.5	6.0±1.5	6.2
<b>1.7±0.3</b>	12.4±0.8	4.0±0.5	7.2
<b>2.0</b>	24.1±6.9	5.8±1.0	12.2

### 4.3.2 Deposition of fibers on silanized substrate and annealed at lower temperature (60°C).

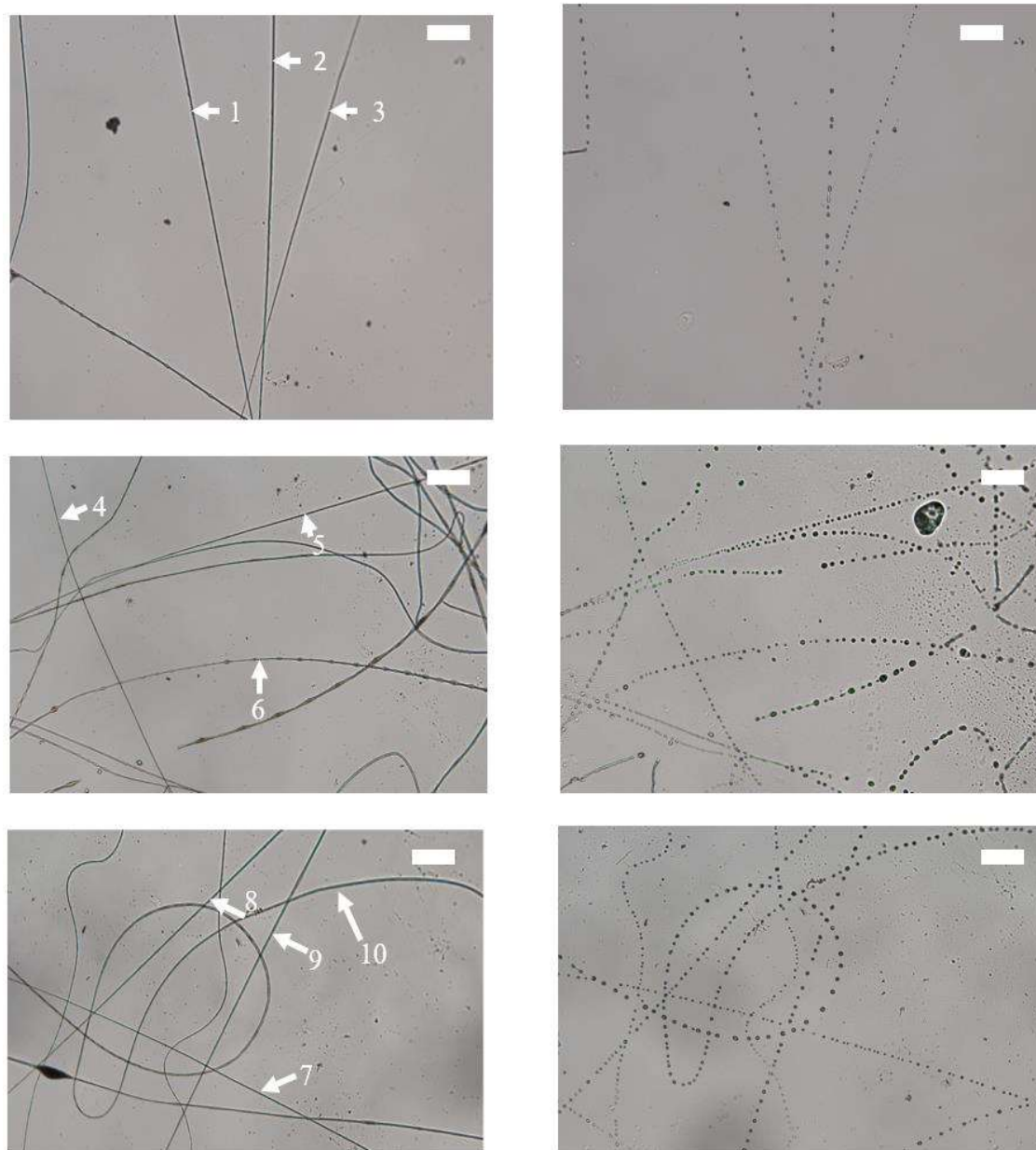


**Figure 30:** In-situ dewetting of nanofibers on silanized substrate and annealed at lower temperature (60°C). (Scale:20 $\mu$ m)

**Table 6:** Length-scale parameters dewetting of nanofibers on silanized substrate and annealed at lower temperature (60°C).

<b>Fiber Diameter(d)/ <math>\mu\text{m}</math></b>	<b>Wavelength(<math>\lambda</math>)/ <math>\mu\text{m}</math></b>	<b>Droplet diameter/ <math>\mu\text{m}</math></b>	<b><math>\lambda/d</math></b>
<b>2.7<math>\pm</math>0.2</b>	11.6 $\pm$ 0.8	4.1 $\pm$ 0.5	4.3
<b>3.2<math>\pm</math>0.3</b>	14.0 $\pm$ 2.8	3.9 $\pm$ 0.2	4.4
<b>3.0<math>\pm</math>0.6</b>	8.7 $\pm$ 1.0	2.2 $\pm$ 0.5	2.9
<b>1.6<math>\pm</math>0.3</b>	8.6 $\pm$ 0.9	3.1 $\pm$ 0.4	5.4
<b>2.1<math>\pm</math>0.5</b>	7.1 $\pm$ 1.420	4.3 $\pm$ 1.0	3.3
<b>1.7<math>\pm</math>0.3</b>	10.9 $\pm$ 1.7	3.1 $\pm$ 0.5	6.2
<b>1.5<math>\pm</math>0.1</b>	9.1 $\pm$ 1.5	2.6 $\pm$ 0.3	6.0
<b>2.2<math>\pm</math>0.3</b>	9.6 $\pm$ 0.6	4.2 $\pm$ 0.5	4.4
<b>2.2<math>\pm</math>0.2</b>	13.7 $\pm$ 1.3	4.5 $\pm$ 0.6	6.1
<b>2.3<math>\pm</math>0.3</b>	10.8 $\pm$ 1.0	4.0 $\pm$ 0.6	4.6

### 4.3.3 Deposition of fibers on unsilanized substrate and annealing at a higher temperature (120°C).

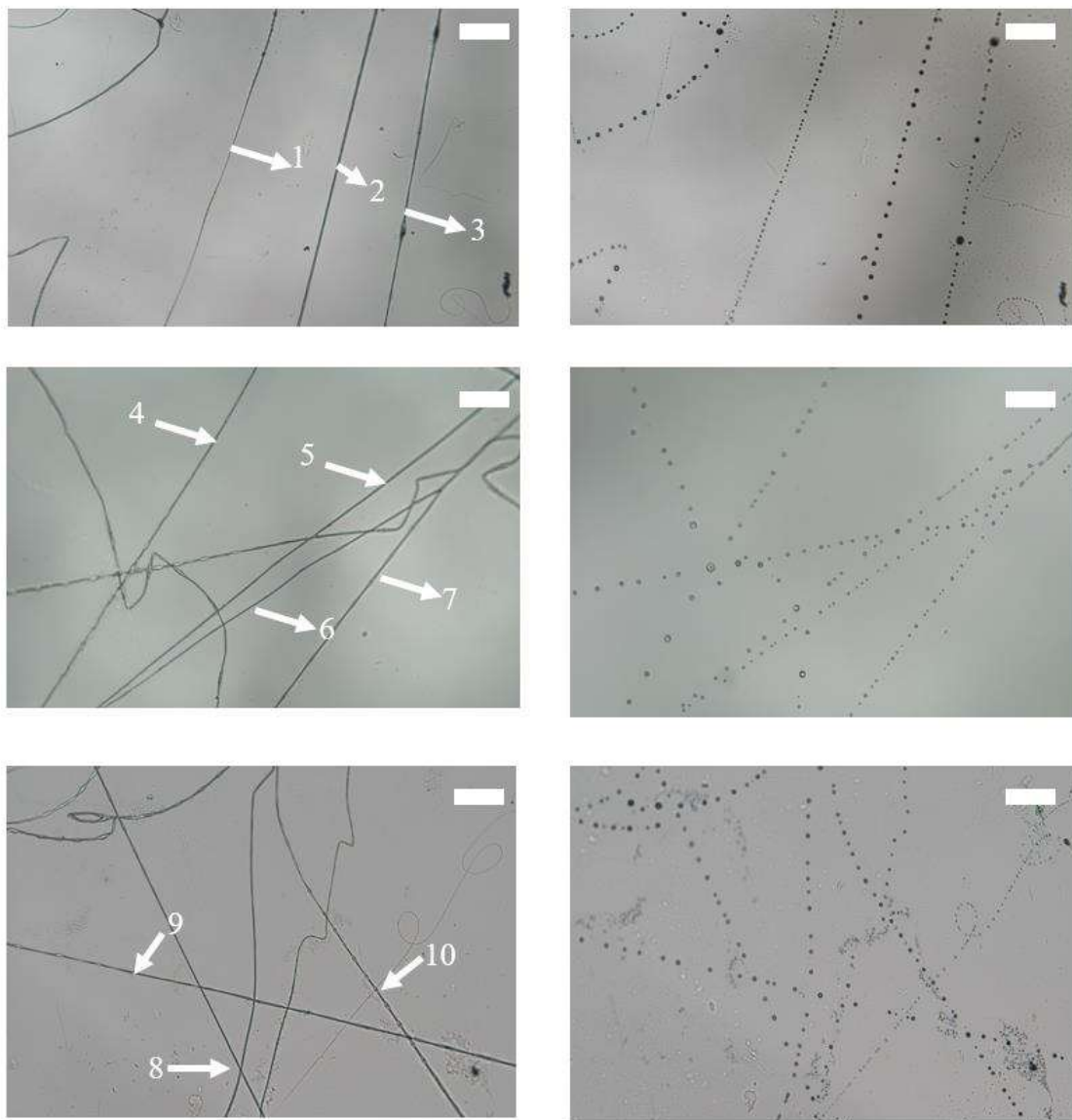


**Figure 31:** In-situ dewetting of nanofibers on unsilanized substrate and annealing at a higher temperature (120°C). (Scale:20 $\mu$ m)

**Table 7:** Length-scale parameters for dewetting of nanofibers on unsilanized substrate and annealing at a higher temperature (120°C).

<b>Fiber diameter(d)/<math>\mu\text{m}</math></b>	<b>Wavelength(<math>\lambda</math>)/ <math>\mu\text{m}</math></b>	<b>Droplet diameter/ <math>\mu\text{m}</math></b>	<b><math>\lambda/d</math></b>
<b>2.7±0.4</b>	6.9±0.5	4.2±0.6	2.5
<b>4.4±0.7</b>	19.0±0.6	5.8±0.5	4.3
<b>3.5±0.6</b>	11.4±1.6	4.0±0.7	3.2
<b>2.5±0.2</b>	24.7±7.7	4.2±0.5	9.7
<b>2.7±0.3</b>	20.0±2.8	3.7±0.5	7.3
<b>2.5±0.4</b>	14.0±1.0	3.8±0.5	5.7
<b>3.9±0.5</b>	11.1±0.6	3.9±0.4	2.8
<b>3.0±0.7</b>	19.3±2.6	3.9±0.3	6.3
<b>1.8</b>	20.5±1	4.0±0.6	11.6
<b>2.9±0.8</b>	13.8±2.0	4.2±0.3	4.7

#### 4.3.4 Deposition of fibers on silanized substrate and annealing at a higher temperature (120°C)

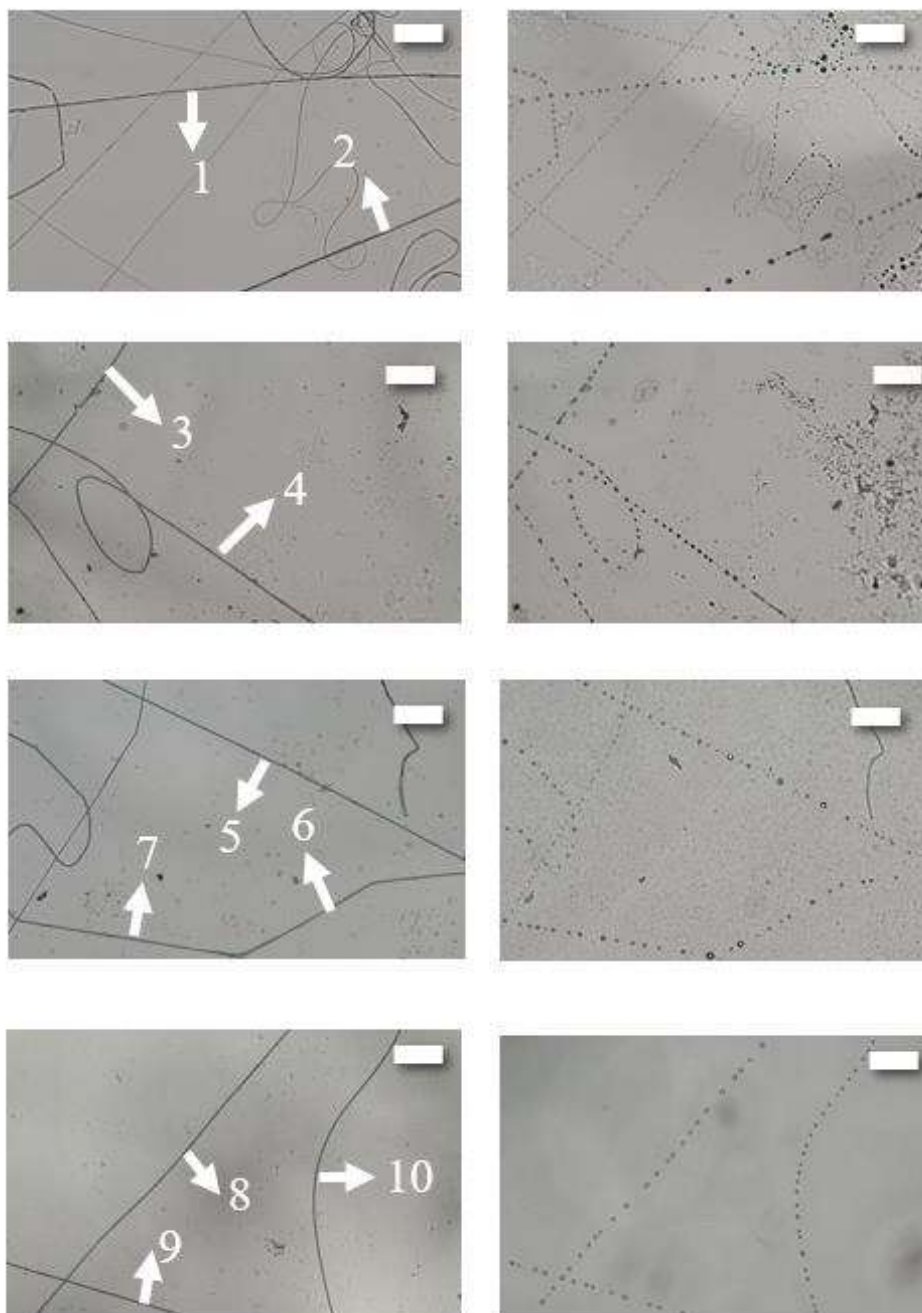


**Figure 32:** In-situ dewetting of nanofibers on silanized substrate and annealing at a higher temperature (120°C) (Scale: 20 $\mu$ m)

**Table 8:** Length-scale parameters for dewetting of nanofibers on silanized substrate and annealing at a higher temperature (120°C).

<b>Fiber diameter/ <math>\mu\text{m}</math></b>	<b>Wavelength/ <math>\mu\text{m}</math></b>	<b><math>\lambda/d</math></b>
1.6 $\pm$ 0.5	5.6 $\pm$ 0.7	3.6
1.9 $\pm$ 0.9	7.0 $\pm$ 0.8	3.7
2.0 $\pm$ 1.0	11.5 $\pm$ 0.5	5.6
2.8 $\pm$ 0.5	14.0 $\pm$ 0.1	4.9
2.4 $\pm$ 0.2	8.8 $\pm$ 0.5	3.7
2.6 $\pm$ 0.9	12.1 $\pm$ 0.7	4.6
2.3 $\pm$ 0.6	13.4 $\pm$ 0.9	5.7
3.5 $\pm$ 0.7	23.9 $\pm$ 0.6	6.7
3.0 $\pm$ 0.5	19.6 $\pm$ 0.7	6.5
3.2 $\pm$ 0.6	21.5 $\pm$ 0.8	6.7

### 4.3.5 Comparison with Rayleigh-Plateau instability model

As the solvent evaporates during electrospinning and solid fibres are produced, the electrospun polystyrene fibres are loosely dispersed over the substrate surface and only make contact with it in a few locations. Each fiber's diameter was measured along its length at ten random locations. Using the standard deviation of the average values generated from these 10 diameter measurements of the fibres, the error was computed. The Rayleigh instability develops when a cylindrical liquid column experiences sinusoidal disturbances with wavelengths longer than the column circumference, which reduce the liquid's surface area and render the column unstable.

When nanowires have a high surface-to-volume ratio and the annealing temperature is considerably lower than the melting point, surface diffusion is primarily responsible for atomic movement that leads to morphological evolution in nanowires. The gradient in the chemical potential caused by a change in the rod's radius is what causes cylindrical rods to become unstable. And in our study, immersion of nanofibers in water-solvent dewetting mixture, provided this perturbation. An approach for structuring long chains of nanospheres is provided by the Rayleigh instability applied to nanowires. This technique should be useful for structuring large surfaces and suitable to a wide range of materials.

According to the Rayleigh-Plateau instability, the value of  $\lambda/d$  should be constant. However, in our case it is more complicated because the surface is also playing an important role in determining this.

### 4.3.6 Multiple times dewetting

The fibres break into droplets after immersing the nanofibers in water-solvent dewetting mixture. The contour of droplets is following the contour of fibers. As nanofibers are deposited on clean substrates and dewetted under optimal dewetting mixture. After this, again nanofibers are deposited on previously dewetted substrates and are dewetted under optimal dewetting solution. This process increases the number density of the dewetted droplets. This can be seen in figure 33.

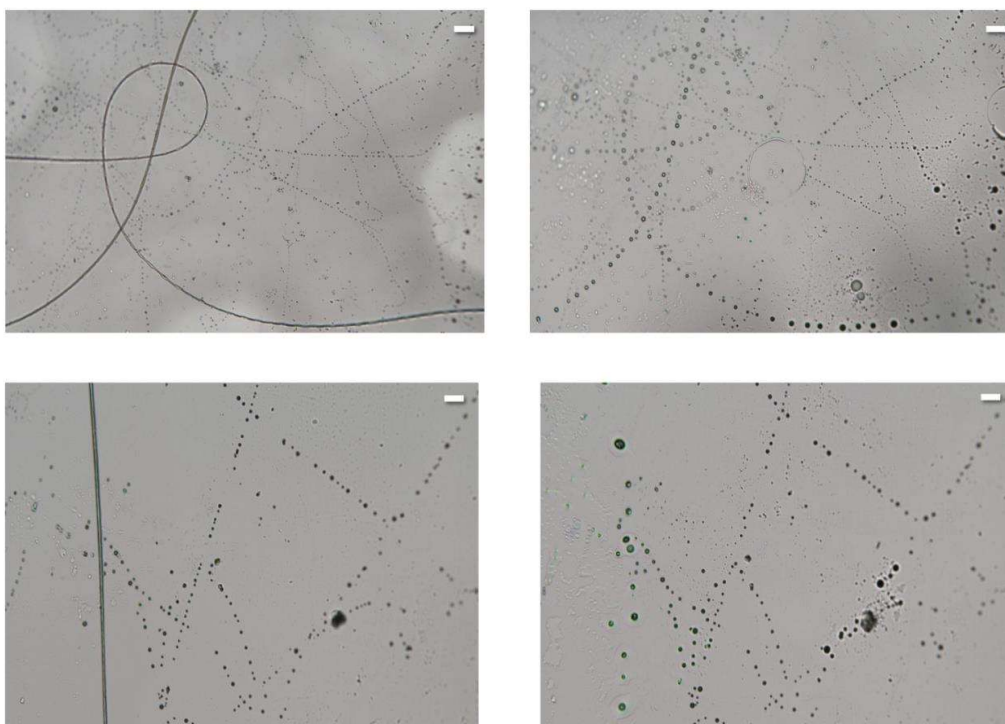


**Figure 33:** Dewetting of nanofibers on previously dewetted substrates

### 4.4 Conclusion

The fibers dewett when kept under the optimal mixture of solvent and water. Previously, 2D structures such as thin films were used that produced random structures. Here, 1D configuration i.e., nanofibers are used instead of 2D structures to get more aligned droplets. The fibers are

coated and dewetted again after first time coat and dewett to get more density of fibers. The density of dewetted droplets cannot be increased in the case of thin films. The  $\lambda/d$  ratio of the dewetted fibers are calculated and its comparison with the Rayleigh-instability model is made.

## References

- [1] Bandyopadhyay, D., Sharma, A., Shankar, V., 2008. Instabilities and pattern miniaturization in confined and free elastic-viscous bilayers. *The Journal of chemical physics* 128(15), 154909.
- [2] Venugopal, J., Ramakrishna, S., 2005. Applications of polymer nanofibers in biomedicine and biotechnology, *Appl. Biochem. Biotechnol.* 125 (3), 147–157.
- [3] Stachewicz, U., Qiao, T., Rawlinson, S.C.F., Almeida, F.V., Li, W.Q., Cattell, M., Barber, A.H., 2015. 3D imaging of cell interactions with electrospun PLGA nanofiber membranes for bone regeneration. *Acta Biomater.* 27, 88–100.
- [4] Zhang, P., Zhao, X., Zhang, X., Lai, Y., Wang, X., Li, J., Su, Z., 2014. Electrospun doping of carbon nanotubes and platinum nanoparticles into the  $\beta$ -phase polyvinylidene difluoride nanofibrous membrane for biosensor and catalysis applications. *ACS applied materials & interfaces* 6(10), 7563-7571.
- [5] Rein, D. M., Cohen, Y., Lipp, J., Zussman, E., 2010. Elaboration of Ultra-High Molecular Weight Polyethylene/Carbon Nanotubes Electrospun Composite Fibers. *Macromolecular Materials and Engineering* 295(11), 1003-1008.
- [6] Shin, Y.M., Hohman, M.M., Brenner, M.P., Rutledge, G.C., 2001. Electrospinning: a whipping fluid jet generates submicron polymer fibers. *Appl. Phys. Lett.* 78 (8), 1149–1151.
- [7] Toimil-Molaes, M.E., Balogh, A.G., Cornelius, T.W., Neumann, R., Trautmann, C., 2004. Fragmentation of nanowires driven by Rayleigh instability. *Appl. Phys. Lett.* 85(22), 5337–5339.

- [8]Dijksman, J.F., Duineveld, P.C., Hack, M.J.J., Pierik, A., Rensen, J., Rubingh, J.E., Schram, I., Vernhout, M.M., 2007. Precision ink jet printing of polymer light emitting displays. *J. Mater. Chem.* 17 (6),511–522.
- [9]Grace, J.M., Marijnissen, J.C.M.,1994. A review of liquid atomization by electrical means, *J. Aerosol Sci.* 25 (6),1005–1019.
- [10]Yurteri, C.U., Hartman, R.P.A., Marijnissen, J.C.M., 2010. Producing pharmaceutical particles via electrospraying with an emphasis on nano and nano structured particles - a review. *KONA Powder Particle J.* 28,91–115.
- [11]Stachewicz,U., Dijksman, J.F., Yurteri, C.U., Marijnissen, J.C.M., 2010. Volume of liquid deposited per single event electrospraying controlled by nozzle front surface modification. *Microfluid. Nanofluid.* 9 (4–5),635–644.
- [12] Stachewicz, U., Yurteri, C.U., Marijnissen, J.C.M., Dijksman, J.F.,2009. Stability regime of pulse frequency for single event electrospraying. *Appl. Phys. Lett.* 95 (22),224105-224108.
- [13]Plateau J.,1873. *Transl. Annual Reports of the Smithsonian Institution.*1863.
- [14]Lord Rayleigh, *Proc. London Math. Soc.* 10, 4,1878.
- [15]Hohman, M.M., Shin, M., Rutledge, G., Brenner, M.P.,2001. Electrospinning and electrically forced jets. I. Stability theory. *Physics of Fluids* 13(8),2201-20.
- [16]Subbiah, T., Bhat, G. S., Tock, R. W., Parameswaran, S., Ramkumar, S. S., 2005. Electrospinning of nanofibers. *Journal of applied polymer science* 96(2), 557-569.